On the Sensitivity of a Tool–Workpiece Thermocouple to Chemical Composition and Microstructure

Philipp Tröber,* Alfred Hackl, Harald Leitner, Markus Welm, Peter Demmel, Matthias Golle, and Wolfram Volk

Meeting the increasing demands on part quality and profitability of manufacturing processes despite difficult-to-machine materials is only possible with a deep understanding of the process. Herein, knowledge about the process temperature is of critical importance since it affects the material properties, such as hardness or forming behavior, as well as the chemical and physical interactions between the tool, workpiece, and lubricant. A proven thermoelectric method of temperature measurement in machining, forming, and blanking is a tool–workpiece thermocouple. Herein, instantaneous measurement of the temperature development is allowed in this setup during the manufacturing process in situ at the contact area of the tool and workpiece. The accuracy of this method is dependent on the calibration of the thermocouple, for which the Seebeck coefficients of the tool and workpiece material have to be determined. Usually, material samples from different batches are used for this purpose, although the resulting measurement errors due to slight changes in material properties are hardly known. The effects of small changes in the chemical composition and the transformation of the crystal lattice due to hardening on the Seebeck coefficient are investigated for the first time to allow precise quantification of the measurement error resulting from the calibration process.

1. Introduction

Since almost all mechanical, electrical, magnetic, and optical material properties depend on temperature, it is generally considered to be one of the most important and most frequently determined technical–physical measurand.[1] During metal processing, the dissipation of up to 95% of the conducted plastic work and friction cause a temperature rise in the workpiece and the active elements of the tool, which effects the whole process.[2] In addition to the mechanical material properties, such as hardness or forming behavior, the resulting temperature influences fundamental physical and chemical interactions between tool, workpiece, and lubricant.[3] Therefore, it determines the lubricant and coating performance, wear behavior, component quality, and process stability. To get a deep understanding of the process and avoid economic losses, especially in mass-production processes such as blanking or cold forming, a precise knowledge about the occurring process temperature is of decisive importance.

Because of their relevance, arising temperatures have been investigated with various methods for almost all manufacturing processes. However, depending on the measuring method used, mentioned temperatures differ greatly in literature. This can be seen exemplarily in the results gained during blanking, where temperatures derived with embedded thermocouples differ between less than 200[4] and 450 °C,[5] and values from 52[6] to over 500 °C[7] can be found in case of radiation thermometry. The large scatter can mainly be traced back to the frequently missing clear geometric and temporal assignment of the temperatures, and especially unknown measurement uncertainties.[8]

Based on thermoelectric phenomena, one method for measuring temperatures in real time is a tool–workpiece thermocouple. Since the tool itself represents the sensor in this case, a time delay due to heat conduction and transfer can be excluded.[9] It allows a locally defined determination of surface temperatures averaged across the entire contact area of tool and workpiece.[10] By using this setup and a punch with undercuts to limit the contact area between punch and sheet metal to the cutting edge, Demmel et al. measured precise temperature curves with maxima up to 250 °C during blanking fine-grained steel with a thickness of

P. Tröber, M. Welm, W. Volk
Chair of Metal Forming and Casting
Technical University of Munich
Walther-Meißner-Str. 4, 85748 Garching, Germany
E-mail: philipp.troeber@tum.de

A. Hackl, H. Leitner
voestalpine BÖHLER Edelstahl GmbH & Co KG
Mariazeller Str. 25, 8605 Kapfenberg, Austria

P. Demmel
MAN Truck & Bus SE
Dachauer Str. 667, 80995 Munich, Germany

M. Golle
Pforzheim University
Tiefenbronner Straße 65, 75175 Pforzheim, Germany

ⓘD The ORCID identification number(s) for the author(s) of this article can be found under https://doi.org/10.1002/srin.202200456.

4 mm.[11] In other investigations, only 165 °C was determined for the same sheet metal. Due to the use of a cylindrical punch, this difference can be attributed to an increased contact area including colder parts, which decreases the average temperature.[8]

Since this measuring setup is always custom-made and especially adapted to machine, tool, and process, different sources of error must be considered to guarantee a high quality of measurement. Measurement errors occur most often due to insufficient electrical insulation, temperature gradients at the electrical contacts causing spurious voltages, and, most importantly, the calibration process.[12–14] For a confidence level of 95%, Demmel calculated an expanded uncertainty of 4 °C in a temperature range between 200 and 300 °C as well as less than 6 up to 400 °C for the whole measuring system.[11] Masek et al. specified an uncertainty of 16.7 °C for their setup in turning.[15]

In regards to the calibration, for geometric reasons, the active elements can often not be characterized directly, and therefore specimens made of the same material are used as substitutes. Furthermore, when using this technology for process monitoring, not all sheet metal batches are thermoelectrically characterized. This causes a measurement error due to variations in the chemical composition, which is negligible with a maximum of 0.3% according to Xu and Tong.[16] However, the respective extent of the influence of individual alloying elements is still unclear. For this reason, the proportions of the elements silicon, aluminum, and nickel in the chemical composition of two different chromium steels were varied and the effect on the thermoelectric behavior of the respective alloy was examined in soft-annealed, as well as hardened and tempered, condition. Afterward, the temperature occurring during blanking was measured. By linking both results, the resulting temperature deviation for a tool–workpiece thermocouple could be quantified.

2. Experimental Setup and Approach

2.1. Tool–Workpiece Thermocouple

A tool–workpiece thermocouple can be implemented in almost all tools without affecting the process. Like standard thermocouples, this method is based on the Seebeck effect, due to which electricity arises in an electrical circuit consisting of two different electrical conductors, when both junctions exhibit different temperatures.[17] Its strength depends on both the temperature difference between the conductor ends and the thermoelectric behavior of the conductors, represented by the Seebeck coefficient.

For this study, this measuring principle, as illustrated in **Figure 1**, was implemented in a stiff and modular blanking tool. Punch and sheet metal represent two different conductors, forming the two legs of the thermocouple. The contact area between both of them represents the measuring junction. Undercuts on the lateral surface of the punch guarantee a defined and localized contact at the cutting edge of the punch.[18] Since common steel alloys do not exhibit high Seebeck coefficients, occurring thermovoltages are very low, in the range of a few millivolts. For this reason, punch and sheet metal are connected to an amplifier and a voltmeter via copper wires. These junctions are located at areas with constant temperature to avoid spurious
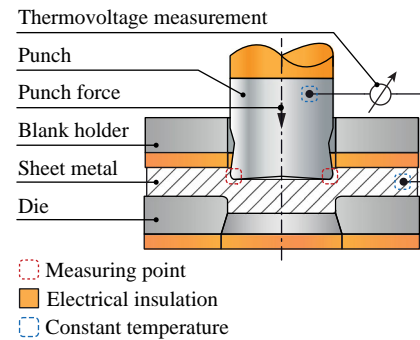
Figure 1. Principle structure of the tool–workpiece thermocouple. Adapted with permission.[18] 2012, Wiley-VCH.

thermovoltages. An electrical insulation of the active elements and the sheet metal from the rest of the tool by ceramic elements prevents interfering signals from the outside. The circular punch has a diameter of 70 mm and a cutting edge radius of 10 μm in all the experiments. No lubricants have been applied. The exact punch geometry, as well as more details, can be found in ref. [11].

2.2. Thermoelectric Material Characterization

A calibration of the tool–workpiece thermocouple is needed to deduce a temperature from the measured thermovoltage. Therefore, both sheet and tool material are characterized with regard to their thermoelectric behavior. This is represented by the thermovoltage curve related to temperature. The slope of this graph corresponds to the material-specific Seebeck coefficient, which is mainly determined by the chemical composition. However, since it depends on a variety of other factors, such as heat treatment state, degree of deformation, and temperature, a thermoelectric characterization can only be performed experimentally.[19] For this reason, a special test setup was developed, whose underlying electrical circuit is shown in **Figure 2**. It consists of the material sample and the reference material platinum, with which a relative Seebeck coefficient is determined.

The characterization process is based on a defined temperature gradient along the specimen, which has a diameter of 10 mm and a length of 160 mm. While one end is kept at a temperature of 0 °C by an ice bath, the other end is continuously heated up to 500 °C. The use of a copper block with heating cartridge ensures uniform heating. Two high-precision thermocouples monitor the temperatures at each end of the sample. They exhibit a diameter of 0.25 mm, which minimizes time delay due to heat transfer. Simultaneously, the arising thermoelectric voltage is amplified und measured. An argon atmosphere prevents measurement errors due to oxidation. By characterizing both legs of a standardized type K thermocouple, a maximum measurement deviation of 1.25% (standard deviation [SD] = 0.5%) of the thermovoltage value could be revealed.

After characterizing all materials relative to platinum, the thermoelectric behavior of the tool–workpiece thermocouple corresponds to the difference between the thermoelectric voltage curves of the tool and workpiece materials. The resulting graph allows the assignment of an exact temperature to each voltage value.
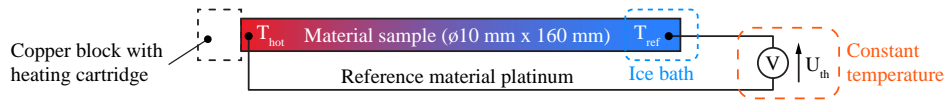
Figure 2. Underlying circuit for the thermoelectric material characterization. Adapted with permission.[19] 2013, Trans Tech Publications Ltd.

Further details on the calibration process can be found in refs. [8,12].

2.3. Investigated Materials in the Basic Chemical Composition

Two 8% chromium steels with only slight differences in their chemical composition, which can be found in **Table 1**, were chosen as basic compositions. While one alloy is conventionally melted (CM) in series production, the other is produced by the electro-slag remelting method (ESR), ensuring low micro- and macro-segregations as well as high purity and homogeneity. In regard to the differing melting processes, these cold-working steels (CWS) will be referred to as CWS_{CM} and CWS_{ESR} in the following sections.

Based on these basic chemical compositions, the quantities of the alloying elements silicon, nickel, and aluminum were varied to determine the effect of variations in their chemical composition on the thermoelectric behavior and thus the measurement accuracy of the tool–workpiece thermocouple. All laboratory materials (LM) were thermoelectrically characterized in the soft-annealed condition as well as after a hardening and tempering process. In addition to these tool steels, the cemented carbide CF–H40S was chosen for temperature measurements during blanking due to its negative Seebeck coefficient. The chosen elements were also characterized separately. All samples exhibited a purity of at least 99.9%.

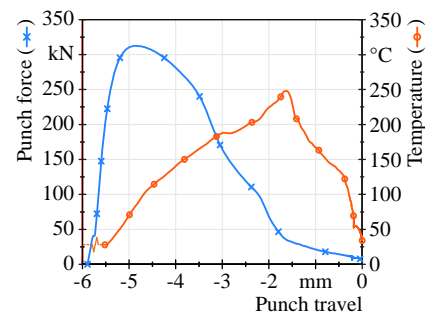The steel grade 42CrMo4 with a thickness of 4 mm was used as sheet metal during the temperature measurement. This common chromium–molybdenum steel is usually used in the automotive industry after being quenched and tempered. The sheets have a tensile strength of 483 MPa and a yield strength of 269 MPa. Table 1 shows the chemical composition of all tool and sheet materials, as well as the modified samples, which were all determined by optical emission spectroscopy with the Foundry-Master from Worldwide Analytical Systems AG, Uedem, Germany. In this method, the material is first vaporized by a spark. Afterward, the chemical composition is derived from the wavelength spectrum of the emitted radiation.

3. Results and Discussion

3.1. Temperature Measurement during Blanking

Figure 3 shows the punch force and temperature profile related to the punch travel during blanking 42CrMo4 with 4 mm thickness. The die clearance was set to 0.04 mm and the punch velocity to $70\,mm\,s^{-1}$. Negative punch travel values indicate a punch movement downward to bottom dead center at 0 mm. The return stroke is not shown because of a missing contact between punch and sheet metal due to the punch geometry.

At −6 mm, the punch gets in contact with the sheet metal and both deform elastically. In this phase, a leveling of asperities takes place resulting in weak heating and a strongly fluctuating signal due to undefined contact conditions. At −5.5 mm, a clear temperature signal arises. Its starting level is 28 °C (SD = 4 °C), corresponding to the ambient temperature. This indicates the beginning of the plastic deformation of the sheet metal, where a defined contact between punch and sheet metal prevails. Subsequently, the punch force grows until its maximum of 313 kN, causing a temperature rise to 103 °C (SD = 1 °C) at −4.6 mm. After the punch force maximum, cracks develop and propagate in the sheet metal, causing a decreasing force. In contrast, temperature still rises almost linearly, but with a smaller slope, until it reaches a plateau at 188 °C (SD = 3 °C)

Table 1. Chemical composition of the investigated materials in mass fraction in %.

	C	Si	Mn	Co	Cr	Mo	WC	V	Ni	Al	Fe
CWS_{ESR}	1.2	0.8	0.4	–	8.1	2.0	–	0.5	0.3	1.0	Balance
CWS_{CM}	1.1	0.7	0.4	–	8.1	2.1	–	0.5	0.2	0.2	Balance
CF-H40S	–	–	–	11.8	–	–	Balance	–	–	–	–
LM_Al_1	1.2	0.7	0.4	–	8.0	2.1	–	0.5	0.3	1.1	Balance
LM_Al_2	1.1	1.0	0.4	–	8.0	2.0	–	0.5	0.3	1.3	Balance
LM_Al_3	1.2	1.0	0.4	–	8.1	2.1	–	0.5	0.3	1.6	Balance
LM_Si_1	1.2	0.5	0.4	–	8.1	2.2	–	0.5	0.2	0.1	Balance
LM_Si_2	1.1	0.9	0.4	–	8.1	2,1	–	0,5	0.3	0.3	Balance
LM_Si_3	1.1	1.3	0.4	–	8.1	2.1	–	0.5	0.3	0.2	Balance
LM_Si_4	1.1	1.5	0.3	–	8.1	2.1	–	0.5	0.3	0.2	Balance
LM_Ni_1	1.2	0.9	0.4	–	8.0	2.0	–	0.4	0.5	< 0.1	Balance
LM_Ni_2	1.1	1.0	0.4	–	8.1	2.0	–	0.4	1.0	< 0.1	Balance
LM_Ni_3	1.1	0.9	0.4	–	8.1	2.0	–	0.4	1.5	< 0.1	Balance
LM_Ni_4	1.1	0.9	0.4	–	7.5	2.0	–	0.4	2.0	< 0.1	Balance
42CrMo4	0.4	0.2	0.7	–	1.0	0.2	–	–	0.1	–	Balance

Figure 3. Punch force and temperature profile over punch travel when blanking 4 mm 42CrMo4 with a die clearance of 1% and a punch velocity of $70\,mm\,s^{-1}$.

**ADVANCED
SCIENCE NEWS**
www.advancedsciencenews.com

**steel
research**
international

www.steel-research.de

at −2.9 mm. This course can be traced back to a partial material separation, which also manifests itself in a change of the punch force slope. Due to the small die clearance, cracks in the sheet metal originating from die and punch do not meet directly, which leads to a renewed formation of clean cut, the secondary clean cut. Together with a localization of the dissipated plastic work in the small, and further declining, shear zone between punch and die, the temperature rises again to its maximum of 248 °C (SD = 5 °C) at −1.6 mm. After the temperature maximum, the sheet metal is separated completely, causing the temperature to decline. In this phase, the cooling of the slug in the die is superimposed by heat introduced by friction between slug and die.

3.2. Chemical Compositions and Thermovoltage

Figure 4 shows the material-specific thermovoltage of the sheet material 42CrMo4, the basic material CWS_{ESR} in hardened and tempered condition, as well as CWS_{CM} in soft-annealed condition with respect to temperature. Furthermore, the figure illustrates the calibration profile of a tool–workpiece thermocouple consisting of CWS_{ESR} and 42CrMo4, which corresponds to the difference between the thermovoltages of both materials. Due to similar thermoelectric behaviors, the resulting calibration curve is low with a maximum of 1.34 mV at 360 °C. It serves as a basis for calculating a real temperature measurement error from the thermoelectric voltage change due to modified chemical compositions. Therefore, the determined deviation is added to the thermoelectricity value of the tool material at 248 °C. With this differing value, a temperature can be determined on the basis of the calibration curve, which shows the temperature deviation. All thermoelectricity curves are averaged over at least five measurements. The highest standard deviation amounts to 0.03 mV in the temperature range from 0 to 300 °C and 0.1 mV up to 500 °C.

Comparing both basic materials, CWS_{CM} generates a thermovoltage, which is 22.5% higher than the one of CWS_{ESR}. This corresponds to a significant difference because most of the alloying elements and therefore steel alloys generate thermovoltages in the range of 3–11 mV relative to platinum.

Due to the strong influence on the material-specific thermovoltage, this difference can be attributed to the chemical composition, which mainly differs in the aluminum and silicon content. Especially the latter is interesting in regard to thermoelectricity.

Due to its semiconductor properties, silicon can generate both negative and positive thermovoltages relative to platinum, depending on the doping element. A high thermovoltage is also characteristic of semiconductors, as confirmed by the thermoelectric characterization of silicon wafers. While boron-doped crystalline silicon generated a maximum thermovoltage of +325 mV (SD = 12 mV) at a temperature of 300 °C, it is −422 mV (SD = 3 mV) with phosphorous at 500 °C.

Therefore, silicon was varied first. **Figure 5** shows the thermovoltages of both basic alloys and the LMs from LM_Si$_1$ to LM_Si$_4$ relative to the temperature difference along the sample. While the silicon content of the investigated materials varies between 0.5% and 1.5%, the rest of the compositions are nearly identical, which can be seen in Table 1. Nevertheless, the results show that increasing the silicon content from 0.5% (LM_Si$_1$) to 1.5% (LM_Si$_4$) lowers the thermoelectric voltage at 500 °C from 8.9 mV (SD = 0.1 mV) to 6.6 mV (SD = 0.1 mV), which corresponds to a reduction of 26.7%.

The smallest change in silicon content between LM_Si$_2$ and LM_Si$_3$ reduces the thermovoltage by 6.1% at 248 °C. In regard to the temperature measurement, an increase of the thermovoltage of the tool material would lower the calibration curve. Consequently, a temperature of 297 °C instead of 248 °C would be measured.

However, CWS_{ESR} still exhibits the lowest thermovoltage, despite a lower silicon content. Since the aluminum content is the other main difference between both basic materials, its amount was varied in the chemical composition of CWS_{ESR}. The resulting thermovoltages are illustrated in **Figure 6**. Although the thermovoltage of pure aluminum is low with a maximum of 3.9 mV (SD = 0.1 mV) at 500 °C compared to silicon, a change in its content has a strong effect on the thermovoltage of the steel alloy. While a difference in the silicon content of about 0.2% between CWS_{CM} and LM_Si$_2$ reduced the thermoelectric voltage by 12.4% (Figure 5), it is 17.8% for a reduction of 0.3% in the aluminum content between LM_Al$_2$ and LM_Al$_3$. Consequently, despite completely different thermovoltage curves, silicon and aluminum exhibit a comparable effect on the thermovoltage of the alloy. An estimation of the resulting error based on the thermoelectric voltages of the pure elements is therefore only conditionally possible.

Due to a higher silicon but lower aluminum content, the change in thermovoltage between CWS_{ESR} and the sample
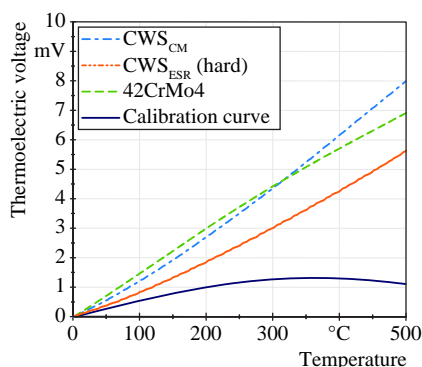

Figure 4. Thermovoltage of the basic materials and the calibration curve for a tool–workpiece thermocouple consisting of CWS_{ESR} and 42CrMo4.
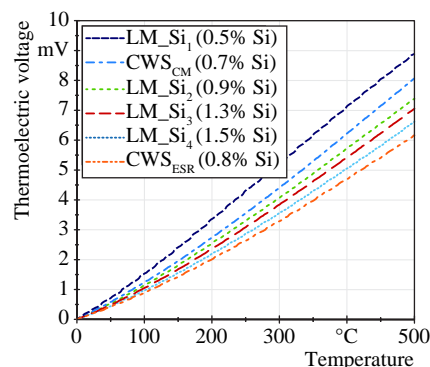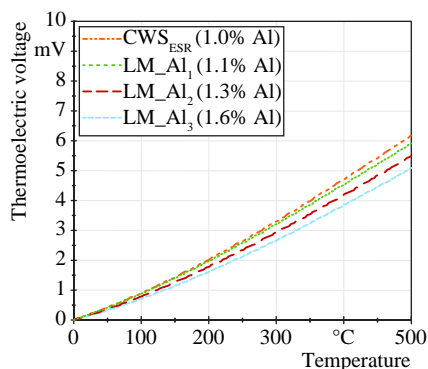

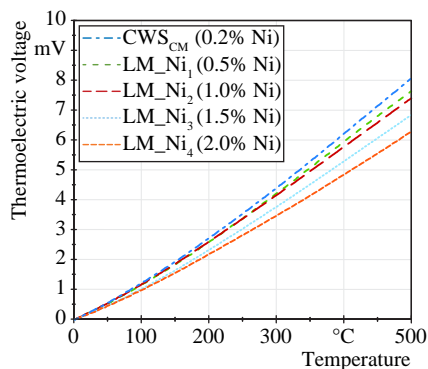**Figure 5.** Effect of variations in the silicon content on the thermovoltage of the alloy.

Figure 6. Effect of variations in the aluminum content on the thermovoltage of the alloy.

material LM_Al$_1$ amounts to 2% at 248 °C. Nevertheless, increasing the thermovoltage of the tool material by this percentage would cause an error in temperature measurement of 18 K.

Nickel was chosen as an element to be varied because it belongs to the few elements with a negative Seebeck coefficient, causing a thermovoltage of -6.1 mV (SD = 0.2 mV) at 500 °C. **Figure 7** illustrates the effect of nickel on the thermovoltage of the basic material CWS$_{CM}$. The thermovoltage profiles indicate that the Seebeck coefficient, and thus the thermovoltage, decreases with an increasing nickel content. A difference in the nickel content of 0.2% between the basic material and LM_Ni$_1$ leads to a reduction in thermovoltage of 5.0%. However, the difference is also influenced by other divergent contents, such as aluminum and silicon. In contrast, the other laboratory samples have a similar composition. While the relative decrease from LM_Ni$_1$ to LM_Ni$_2$ amounts to 2.6%, it is 6.8% from LM_Ni$_2$ to LM_Ni$_3$ and 8.7% from LM_Ni$_3$ to LM_Ni$_4$. In total, 2% more nickel in the composition reduces the thermovoltage by 17.1%. The reduction in thermovoltage between CWS$_{CM}$ and LM_Ni$_1$ of 4.5% corresponds to a measurement error of 35 K.

3.3. Effect of Heat Treatment on the Thermovoltage

Because of the high surface pressures and loads in a blanking tool, active elements are normally hardened and tempered before use. While the hardening process causes a hardness increase due
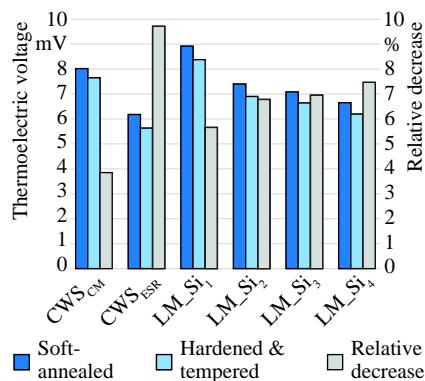
to a structural transformation from austenite to martensite, a subsequent tempering reduces tensions in the structure again, depending on temperature and time, and allows a precise adjustment of the toughness and final hardness. Furthermore, the retained austenite in the structure transforms into martensite, too.

To investigate the resulting effect on the thermoelectric behavior of the alloy, all samples were first examined in the soft-annealed and afterward in the hardened and tempered condition. The heat treatment was carried out for each material according to the manufacturer's specifications. **Figure 8** shows the microsections of the basic materials and the laboratory sample LM_Si$_1$ exemplary for the silicon variation. While all samples exhibit austenite with coagulated carbides in the soft-annealed condition, the material structure changes to fine-tempered martensite after heat treatment. The only difference between the laboratory samples and the basic materials are coarser chromium carbides of the latter. Significant differences in the grain size could not be observed.

Figure 9 illustrates the thermovoltage occurring at a temperature of 500 °C for the basic materials and all samples from the silicon variations in soft-annealed and hardened condition. The relative change of the thermovoltage between both conditions is also given. Across all samples, the transformation of the structure causes a decrease in the Seebeck coefficient and thus a lower
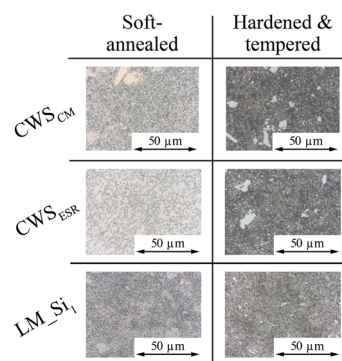
Figure 8. Microsections of the basic materials and LM_Si$_1$ in soft annealed as well as hardened and tempered condition.

Figure 7. Effect of varying nickel content on the thermovoltage of the alloy.

Figure 9. Effect of the hardening process on the thermovoltage at 500 °C.

ADVANCED
SCIENCE NEWS
www.advancedsciencenews.com

steel
research
international
www.steel-research.de

slope of the thermovoltage curve. The highest relative change occurs in case of the basic material CWS$_{CM}$, where the thermovoltage declines from 6.2 to 5.6 mV. This corresponds to a relative change of 9.7%. In contrast, CWS$_{ESR}$ with 3.8% exhibits the smallest relative decrease in thermovoltage across all materials. In sum, despite different levels of thermovoltage, the crystal lattice transformation leads to a similar absolute decrease of 0.5 mV for all LMs, which corresponds to an average relative decrease of 6.7% (SD = 2.0%). Since the chemical composition is the same before and after heat treatment, this change can be attributed to the changes in the crystal structure, especially the transformation from austenite to martensite and the accompanying tensioning of the lattice. This is in accordance with the results of Demmel et al. who found comparable effects of strain hardening on the material-specific thermovoltage.[19] In contrast, a comparison of the thermoelectric voltages of the basic materials with the laboratory samples shows that the size of the carbides after heat treatment plays a subordinate role. Although both basic materials have larger carbides than the laboratory samples, the basic materials show an under- and overcutting of the average.

Altogether, it can be assumed that the influence on the Seebeck coefficient depends on the parameters of the heat treatment and thus the exact structure and lattice characteristics.

If a soft instead of a hard material was used in the thermocouple consisting of CWS$_{ESR}$ and 42CrMo4, this change would correspond to a measurement error of 56 K. While the absolute decrease in thermoelectricity is in accordance with ref. [16], the resulting measurement error deviates strongly compared to 10 K, which can be attributed to the low calibration curve.

4. Conclusion

In this study, the course of the temperature with a maximum of 248 °C (SD = 5 °C) was measured with a tool–workpiece thermocouple during blanking.

Afterward, the proportions of silicon, aluminum, and nickel in the chemical composition in two basic alloys were varied and the effects on the material-specific thermoelectric voltage relative to platinum were investigated. The results show that an increase in the proportion of each of these elements decreases the thermovoltage of the alloy. While increasing the silicon proportion from 0.5% to 1.5% causes the thermovoltage to decrease by 26.7% at 500 °C, the addition of 0.6% aluminum lowered it by 17.8%. In the case of nickel, a decrease of 20% occurs when increasing the content from 0.2% to 2%. The hardening process reduces the thermovoltage by an average of 6.7% across all investigated materials.

Based on the calibration curve of a tool–workpiece thermocouple made out of CWS$_{ESR}$ and 42CrMo4, the smallest occurring changes in thermovoltages due to the chemical composition correspond to a measurement error at 248 °C of 49 K for silicon, 18 K for aluminum, and 35 K for nickel. Ignoring the hardening process would lead to a measurement error of 56 K. These values confirm that changes in chemical composition due to batch fluctuations can lead to a significant measurement error in case of a low calibration curve of the thermocouple.

[1] F. Bernhard, *Handbuch der Technischen Temperaturmessung*, Springer Vieweg, Berlin, Germany **2014**.

[2] G. Taylor, M. Quinney, *Proc. R. Soc. London, Ser. A* **1934**, *143*, 307.

[3] P. Demmel, H. Hoffmann, R. Golle, C. Intra, W. Volk, *CIRP Ann.* **2015**, *64*, 249.

[4] C. Rentsch, Feinschneiden mit beschichteten Werkzeugen: Fort. Ber. VDI, Nr. 413 **1996**.

[5] N. Fischekov, *Wie wirkt der Wärmeeinfluß auf die Standzeit von Stanzwerkzeugen?* Werk. Betr. 124, Carl Hanser Verlag GmbH & Co. KG, Munich **1991**.

[6] S.-H. Kim, J. J. Kang, D.-J. Lee, *AIP Conf. Proc.* **2007**, *7*, 877.

[7] M. Schüßler, *Doctoral Thesis*, Tech. Hochschule Darmstadt **1990**.

[8] P. Tröber, M. Welm, H. A. Weiss, P. Demmel, R. Golle, W. Volk, in *MATEC Web of Conf.*, EDP Sciences, Les Ulis **2018**, p. 190.

[9] T. Junge, H. Liborius, T. Mehner, A. Nestler, A. Schubert, T. Lampke, *Procedia CIRP* **2020**, *93*, 1435.

[10] J. Glascott, F. H. Stott, G. C. Wood, *Philos. Mag. A* **1985**, *6*, 811.

[11] P. Demmel, *Doctoral Thesis*, Technical University Munich **2014**.

[12] P. Tröber, M. Welm, H. A. Weiss, P. Demmel, R. Golle, W. Volk, *Manuf. Rev.* **2019**, *6*, 1.

[13] D. A. Stephenson, *J. Eng. Ind.* **1991**, *2*, 121.

[14] M. C. Santos, Á.R. Machado, M. A. S. Barrozo, L. M. Neto, E. A. A. Coelho, *Measurement* **2013**, *46*, 2540.

[15] P. Masek, P. Zeman, P. Kolar, *Int. J. Adv. Manuf. Technol.* **2021**, *116*, 3163.

[16] H. J. Xu, X. C. Tong, *CIRP Ann.* **1983**, *1*, 47.

[17] M. A. Davies, T. Ueda, R. M'Saoubi, B. Mullany, A. L. Cooke, *CIRP Ann.* **2007**, *56*, 581.

[18] P. Demmel, T. Kopp, R. Golle, W. Volk, H. Hoffmann, *Special Edition: 14th Int. Conf. on Metal Forming* **2012**, pp. 291–294.

[19] P. Demmel, P. Tröber, T. Kopp, R. Golle, W. Volk, H. Hoffmann, *Mater. Sci. Forum* **2013**, *755*, 1.

© 2022 The Authors. Steel Research International published by Wiley-VCH GmbH